ChemMedChem

Accepted Article

Title: Identification of novel fragments binding to the PDZ1-2 domain of PSD-95

Authors: Jie Zang, Fei Ye, Sara Solbak, Lars Jakobsen Høj, Mingjie Zhang, and Anders Bach

Identification of novel fragments binding to the PDZ1-2 domain of PSD-95

Jie Zang,[a] Fei Ye,[b] Sara M. Ø. Solbak,[a] Lars J. Høj,[a] Mingjie Zhang,[b] and Anders Bach*[a]

[a]   Dr. J. Zang, Dr. S. M. Ø. Solbak, Dr. L. J. Høj, Assoc. Prof. A. Bach
        Department of Drug Design and Pharmacology
        Faculty of Health and Medical Sciences
        University of Copenhagen
        Universitetsparken 2, 2100 Copenhagen (Denmark)
        E-mail: anders.bach@sund.ku.dk
[b]   Dr. F. Ye, Prof. M. Zhang
        Division of Life Science
        Hong Kong University of Science and Technology
        Clear Water Bay, Kowloon, Hong Kong (China)

        Supporting information for this article is given via a link at the end of the document.

Abstract: Inhibition of PSD-95 has emerged as a promising strategy for treatment of ischemic stroke as shown with peptide-based compounds that target the PDZ domains of PSD-95. In contrast, developing potent and drug-like small-molecules against the PSD-95 PDZ domains has so far been unsuccessful. Here, we explore the druggability of the PSD-95 PDZ1-2 domain and use fragment screening to investigate if this protein is prone to bind small-molecules. We screened 2,500 fragments by fluorescence polarization (FP) and validated the hits by surface plasmon resonance (SPR) including an inhibition counter-test and found four promising fragments. Three ligand efficient fragments were shown by $^1H-^{15}N$ HSQC NMR to bind in the small hydrophobic P^0 pockets of PDZ1-2, and one of them underwent structure-activity relationship (SAR) studies. Overall, we demonstrate that fragment screening can successfully be applied to PDZ1-2 of PSD-95 and disclose novel fragments that can serve as starting points for optimization towards small-molecule PDZ domain inhibitors.

The neuronal scaffolding protein postsynaptic density protein-95 (PSD-95) forms protein-protein interactions (PPIs) with the *N*-methyl-D-aspartate (NMDA) receptor and neuronal nitric oxide synthase (nNOS) through its PSD-95/Discs-large/ZO-1 (PDZ) domains. Thereby, glutamate-mediated NMDA receptor activation and the resulting Ca^{2+} influx are linked to the production of nitric oxide (NO) by nNOS.[1] During pathological over-activation of NMDA receptors excessive and harmful levels of Ca^{2+} and NO contribute to excitoxicity and cellular damage.[2] The 20-mer peptide Tat-NR2B9c binds the PDZ1 and PDZ2 domains of PSD-95 and is thereby able to inhibit the nNOS/PSD-95/NMDA receptor complex and uncouple NMDA receptor activation from downstream toxic events such as NO production.[2] Tat-NR2B9c has shown neuroprotective effects in several animal stroke models and even in recent clinical stroke trials.[3] Also, high-affinity dimeric peptide-based inhibitors that bind the PDZ1-2 domain of PSD-95 are neuroprotective in mouse and rat stroke models,[4] and other peptide-based PSD-95 inhibitors have shown effects in animal models of pain[5] and neurodegenerative diseases.[6] Since PSD-95 inhibitors do not affect the ion transportation through the NMDA receptor they are believed to be safer drug candidates compared to NMDA receptor antagonists.[2, 7]

Small-molecule inhibitors of PDZ domains could be advantageous over peptide-based compounds as such molecules are generally more permeable to membranes and biological barriers and less prone to cause immunologic reactions, biological degradation, and kidney excretion. However, development of small-molecule PDZ domain inhibitors has proven to be very difficult.[8] Except for Biogen's tripeptide-like nanomolar PICK1 PDZ domain inhibitors,[9] potent (<1 µM) small-molecules are lacking for the ~260 human PDZ domains, including those of PSD-95.[10] A better understanding of PDZ domains and their ligand-binding capabilities could open up for new chemical probes and drug candidates towards a plethora of biological relevant proteins.

Previous assessments using computational and experimental methods deemed PDZ domains non-druggable or non-amenable to small-molecule binding.[11] Noticeably, 11,759 fragments were screened against PSD-95 PDZ1 by $^1H-^{15}N$ HSQC NMR without finding a single hit.[11b] This result was attributed to the structure of the PDZ domain pocket, which is elongated and shallow in shape.[11] These features correlate with the natural role of PDZ domains, which is to interact with the C-terminal peptide parts of their protein interacting partner often with micromolar affinities,[12] but makes small-molecule drug discovery challenging.

Here, we examined the druggability of the PDZ1-2 domain of PSD-95 by computational methods and experimental fragment screening using fluorescence polarization (FP) as screening assay, and surface plasmon resonance (SPR) and $^1H-^{15}N$ HSQC NMR as sensitive methods for validation and characterization of the fragment-protein interactions.

First, an FTMap analysis of PDZ1-2 was conducted. This computational method identifies likely hot spots, i.e. regions of the protein that contribute the most to ligand binding affinity, by sampling a series of small organic probe molecules across the protein and calculating their binding energy. Regions that bind several kinds of probe molecules (consensus clusters, CC) indicate hot spot areas.[13] FTMap identified two main clusters in PDZ1 and PDZ2 of PDZ1-2, respectively, which correlate with the hydrophobic P^0 pockets that are normally occupied by the extreme C-terminal hydrophobic amino acid (often Val or Ile) of the peptide ligand (Figure 1).[14] However, the two main clusters (CC1 and CC2) are rather small and very far apart, and the
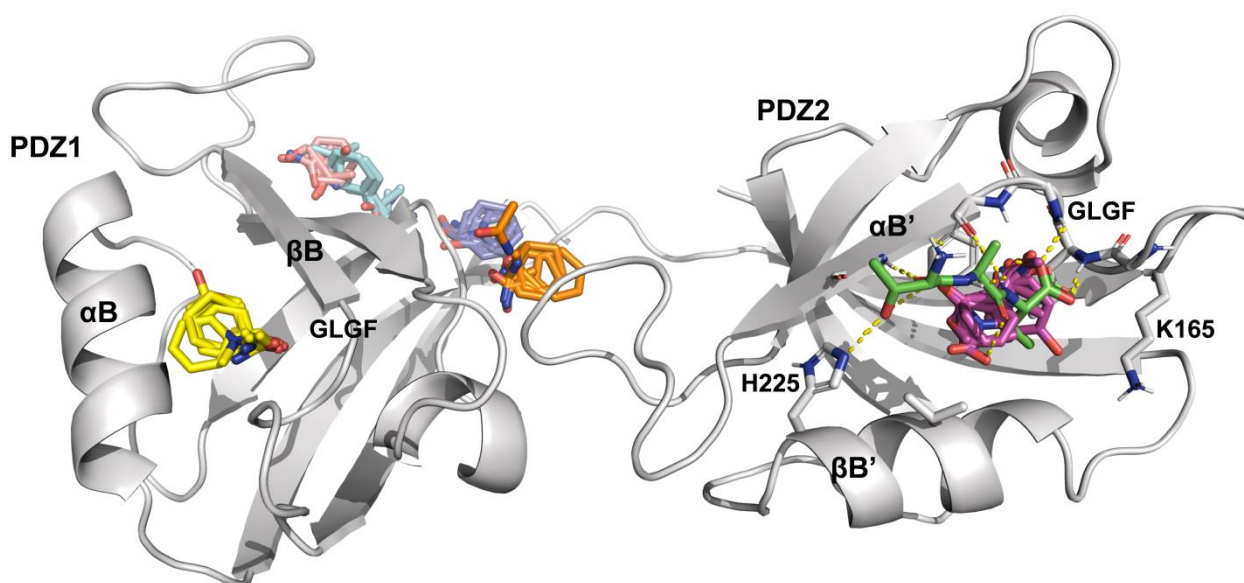
Accepted Manuscript

Figure 1. FTMap results showing two consensus clusters (CC1–2) in PSD-95 PDZ1-2. Consensus cluster strength (S) is defined as the number of probe clusters within the consensus cluster. CC1 is found in the hydrophobic P^0 pocket of PDZ2 (21 probe clusters; maximum dimension is 7.0 Å; magenta sticks) and CC2 is likewise seen in P^0 of PDZ1 (17 probe clusters; maximum dimension is 6.1 Å; yellow sticks). The distance between CC1 and CC2 is 38 Å. Four smaller consensus clusters (containing 7–15 probe clusters) are seen on the other side (salmon, cyan, blue, and orange sticks) and are thus disconnected from CC1–2. Tripeptide TAV (**1**) docked into PDZ2 is shown in green sticks to illustrate typical peptide-PDZ interactions (yellow dashes).

additional even smaller clusters are found on the other side of the protein where ligands normally do not bind (Figure 1). Overall, the absence of secondary hot spots close to CC1/2, the large distance between the hot spots, and their small dimensions makes PDZ1-2 a challenging target for small-molecule drug discovery. However, a previous FTMap analysis of PDZ1 suggested a secondary cluster around the conserved His130 (His225 in PDZ2),[13a] but no experimental evidence for such a potential small-molecule prone hot-spot has been provided.

We next screened our library of 2,500 commercial available 'rule of 3' compliant fragments[15] by our well-established FP competition assay.[4a, 14] This assay measures the ability of the fragments to inhibit the interaction between PDZ domain and a fluorescent-labelled peptide probe derived from the NMDA receptor GluN2B subunit. The assay was optimized for sensitivity towards weak binders by exploring various combinations of PDZ domains (PDZ2 or PDZ1-2 of PSD-95) and Cy5-labelled peptide probes (either a monomeric 11-mer derived from the C-terminus of the NMDA receptor GluN2B subunit,[14] or a high-affinity dimeric probe[4a, 16]) and checked for DMSO tolerability. Tripeptides TAV (**1**) and the corresponding TAV peptide where the amino group was replaced with hydrogen (**2**)[14] were used as weak-affinity inhibitors during optimization. The combination of PDZ1-2 and the monomeric probe gave the lowest IC$_{50}$ values for **1** and **2** (220 and 2600 µM, respectively), and DMSO from 1–8% did not affect the sensitivity of the assay (Figure S1). The 2,500 fragments were then screened at 4 mM (4% DMSO), and 63 fragments showed >10% inhibition and were defined as primary hits (2.5% hit rate). These hits were next validated in dose-response experiments (0.5–8 mM, 0.5–8% DMSO) in the presence and absence of PDZ1-2 in order to identify false-positives related to fluorescence inner-filter effects.[17] Sixteen fragments showed dose-dependent inhibition without a concomitant decrease in FP when PDZ1-2 was omitted from the assay, corresponding to a validated hit rate of

0.6% (Figure 2). Still, the inhibition effects were in most cases small or sometimes showing a sharp dose-dependency.
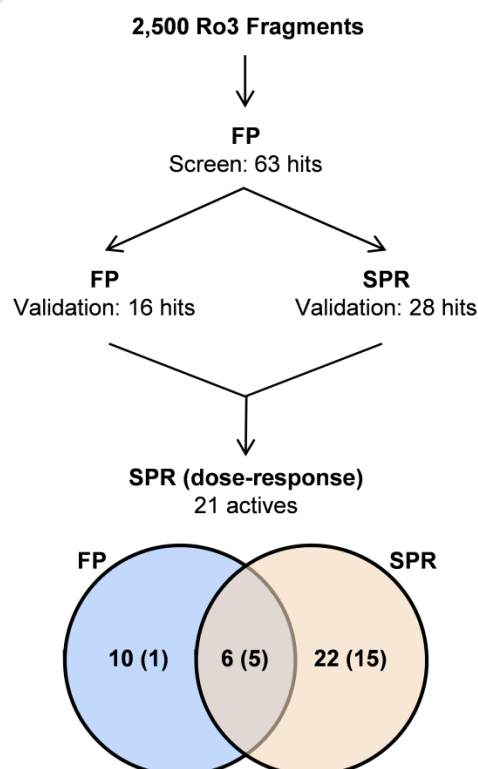

Figure 2. Screening cascade and Venn diagram of our fragment screening campaign against the PSD-95 PDZ1-2 domain. Venn diagram shows number of hits after validation. Numbers in parenthesis indicate how many of the FP/SPR validated hits that also showed dose-dependent and fragment-like binding in the SPR dose-response test.
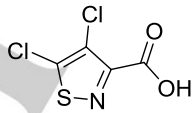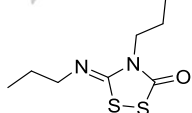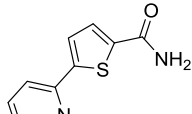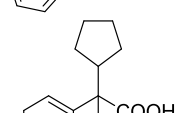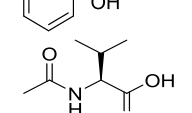
To further characterize the 63 primary FP hits and exclude other types of false positives, such as aggregation-based

promiscuous inhibitors,[18] we conducted a series of SPR validation experiments. SPR is a sensitive technique that can detect direct binding to the protein and unusual sensorgram shapes or response levels above those of comparative control compounds are indicative of false positives.[17, 19] In SPR, the fragments were injected in a OneStep concentration gradient at 0.5 mM and 1 mM (4% DMSO) over immobilized PSD-95 PDZ1-2 in a 384-well plate format. An 8-mer GluN2B-derived peptide (LSSIESDV-OH, **3**[14]) and **2** were used as a positive controls (Figure S2). To discriminate true binding events from non-specific binding and bulk effects, a follow-up counter-test was performed where the running and ligand buffers contained 10 µM of a high-affinity dimeric PDZ1-2 inhibitor (**4**).[20] The affinity of **4** has previously been determined to be 10 nM by ITC (K_d) and FP (K_i);[4a, 20] here a K_d of 21–73 nM was determined by SPR (Figure S2). Thereby, the PDZ1-2 domain binding pocket is blocked by **4** during the counter-test and fragment binding to the site is hindered leading to reduced response.[19, 21] Out of the 63 primary FP hits, 28 were considered SPR validated as they gave a MW normalized response level higher than 40% of the response level of the weak control compound **2** in the primary SPR experiment (**2** and the hits showed response levels around 10 RU and 4–20 RU, respectively). Also, these fragments had an 'S' value ≥0.3, where S is a calculated metric based on the responses from the primary test and the counter-test[21] (S = 0.3 corresponds to a reduction in response level of 50%). Among the 28 SPR validated fragments, six were also FP validated hits (Figure 2). The 38 FP/SPR validated hits were further characterized by a SPR dose-response experiment by injecting the fragments as two-fold serial dilutions (0.125–2 mM, 4% DMSO). This allowed for a more careful evaluation of fragment-like binding behaviour (e.g. fast kinetics and weak affinities) and provided another measurement of the binding affinity to PDZ1-2. Five out of the six fragments that were validated by both FP and SPR showed dose-dependent and fragment-like binding, as did 15 out of the remaining 22 SPR validated hits (Figure 2). Four fragments (**5**–**8**) showed affinities below 10 mM in the dose-response SPR experiment, and these K_d values generally correlated well with those suggested by OneStep SPR injections (Table 1 and Figure S3–4). Interestingly, fragments **5**, **6**, and **8** were also among the pool of hits that were validated in both the FP and SPR validation step (Figure 2). Fragment **7** was FP validated, but, however, not defined as an SPR validated hit (Figure 2) due to a low S value.

The native peptide ligands of PSD-95 PDZ1-2 inserts the side chain of the C-terminal amino acid (most often Val) into the small hydrophobic P[0] pocket while the C-terminal carboxylic acid simultaneously makes hydrogen bonds with the backbone of the conserved Gly-Leu-Gly-Phe (GLGF) motif (Figure 1).[22] Based on the structures of **5**–**8**, we imagined a similar binding mode of these fragments. Thus, to compare the binding efficiencies of **5**–**8** we designed the smallest possible truncation product of the GluN2B peptide ligand, i.e. *N*-acetyl-L-Val (**9**), and tested it by SPR. From this it was clear that the best fragment hits bind with similar (**5**–**7**) or slightly improved (**8**) affinities compared to **9** (Table 1 and Figure S3–4). Notable, the ligand efficiency (LE)[23] of **5** was better than for **9** (0.29 vs 0.27), indicating that **5** fits well into the PDZ domain pocket. For fragment **6**–**8**, LE was lower than **9** (Table 1), but still at a reasonable level considering that PDZ1-2 is a PPI target.

Next, binding of fragment hits **5**–**8** to PDZ1-2 was explored by NMR chemical shift perturbation (CSP) analysis based on ^1H–^{15}N HSQC NMR titration experiments. NMR titration of peptide controls **1** and **3** to PDZ1-2 showed obvious chemical shifts indicating their interaction with PDZ1-2 (Figure S5A-B, E). The slow exchange between the ligand-bound and ligand-free PDZ1-2 in the titration is consistent with the high potency of compound **3** (Figure S5B). Multiple peaks of PDZ1-2 underwent fast exchange upon the binding of fragment **5**, **8** and **9** (Figure 3A-C), indicating their interaction with PDZ1-2. Fragments **6** and **7** only gave negligible chemical shifts (Figure S5C-D). However, **6** was found unstable under the conditions of the NMR experiments and **7** was hampered by low solubility preventing testing at high excess of ligand. Mapping of binding-induced chemical shift changes to the structure of PDZ1-2 suggested that fragment **8** binds to PDZ1-2 by showing fast exchange of chemical shifts specifically at the canonical GLGF loops and hydrophobic P[0] pockets of the βB–αB grooves of PDZ1-2 with PDZ2 showing the strongest signals (Figure 3B, D). This correlated with the suggested binding pose of **8** by molecular docking (Figure 3E). Docking of **5**–**7** and **9** suggested that these were also interacting with PDZ1-2 at these motifs (Figure S6).

Table 1. SPR validation data of fragment hits[a]

F#	Structure	SPR – OneStep (K_d/mM)	SPR – MCI (K_d/mM) (LE)
5		6.2	7.1 (0.29)
6		2.3	7.7 (0.22)
7		2.8	7.3 (0.21)
8		3.2	4.2 (0.20)
9		-	6.3 (0.27)

[a] SPR K_d values of fragment hits **5**–**8** and control fragment **9** as found by OneStep (1 mM) or dose-response multi-cycle injections (MCI) (2-fold serial dilutions) during the validation step (both n=1). LE values shown in parenthesis are based on dose-response K_d values. Sensorgrams are shown in Figure S3–4.

A series of 20 analogues of fragment **8** (**10**–**29**) were purchased or synthesized (Scheme S1) and tested by SPR to gain structural insight of the binding mode of **8** within the PDZ1-2 pockets. From this it became clear that the cyclopentyl group was important for binding as removing it (**10**), increasing or decreasing the alkyl ring (**11**–**12**), or opening (**13**–**15**) or aromatizing (**16**–**17**) it resulted in weaker compounds (Table 2). In the suggested docking pose (Figure 3E), the cyclopentyl
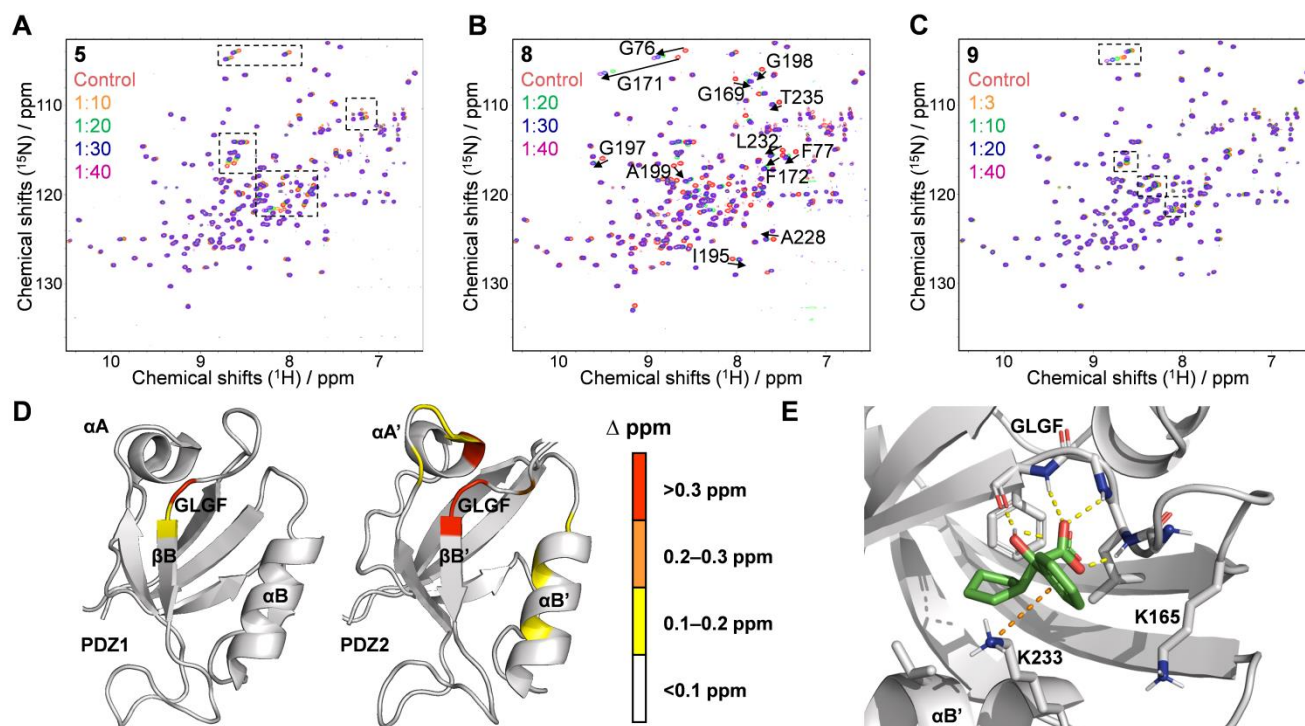
3

Figure 3. A-C) NMR-based titrations of PDZ1-2 with increasing concentrations of fragment hits **5** and **8** and control fragment **9**. ^{1}H,^{15}N HSQC spectra of ^{15}N-labelled PDZ1-2 (150 μM) without or with the respective compounds are shown. D) Mapping of binding-induced chemical shift changes to PDZ1-2 by **8** illustrates that **8** binds to the GLGF loop and P^0 pocket of the conserved βB–αB PDZ binding groove in both PDZ domains. PDZ1 and PDZ2 of PDZ1-2 are presented separately for clarity. The combined ^{1}H and ^{15}N chemical shift changes are defined as $\Delta ppm = [(\Delta\delta_{HN})^2 + (\Delta\delta_N \times \alpha_N)^2]^{1/2}$, where $\Delta\delta_{HN}$ and $\Delta\delta_N$ represent the chemical shift difference. The scaling factor α_N to normalize the ^{1}H and ^{15}N chemical shifts is 0.17. E) Fragment hit **8** (green sticks) docked into PDZ2 of PSD-95. The highest ranking pose is shown of (R)-**8**. Polar contacts are shown in yellow dashes, and a suggested π-cation interaction between **8** and K233 is shown in orange dashes.

group of **8** binds into the P^0 hydrophobic pocket, which is normally occupied by a Val side chain from the native peptide ligand (Figure 1). Apparently, for the small fragment **8**, the cyclopentyl group provides stronger binding than this branched alkyl group. Esterification or amidation of the carboxylic acid of **8**, as in **18**–**19**, led to basically inactive compounds. This correlates with the docking of **8** where the carboxylic acid group forms essential hydrogen bonds to the GLGF motif similar to peptide ligands.[22] Interestingly, the hydroxyl group of **8** also engages in hydrogen bonding to the PDZ GLGF motif according to docking (Figure 3E) - similar to the first amide NH group of the peptide ligand (Figure 1). Accordingly, removing the hydroxyl group led to a much weaker compound (**20**), and so did changes of the central C–OH group into amides or sulfonamides as in **21**–**24** (Table 2). Finally, *ortho* or *para*-substitutions of the phenyl ring of **8** with electron withdrawing or donating groups resulted in **25**–**28** showing clear binding to PDZ1-2 only slightly weaker than **8**. Also, **29** was equipotent to **8** demonstrating that thiophene could replace the phenyl ring (Table 2). In docking, the phenyl ring points towards the αB' helix and forms a π-cation interaction with Lys233 (Figure 3E). This part of the ligand and corresponding protein area could be focus of future optimizations.

In conclusion, we here report a screening campaign testing 2,500 fragments against the PDZ1-2 domain of PSD-95 using FP and SPR as screening and main validation methods. This included counter-tests where PDZ1-2 was omitted from the FP assay to identify fluorescence artefacts, and an SPR step where the target was blocked by a high-affinity ligand. This strategy

facilitated the identification of the most promising hits, which were also confirmed and further characterized by dose-response SPR. Four fragments (**5**–**8**) bound PDZ1-2 with K_d values of 2–8 mM. Although these affinities are low, they are in the same range as the native peptide-derived fragment N-acetyl-L-Val (**9**), and the ligand efficiencies are reasonable to good and comparable to **9**. This indicates a good fit into the binding pocket, and suggests they could provide starting points for further ligand design. Also, fragments **5**–**8** are novel in structure in relation to PDZ domain drug discovery, and can be docked to show binding into the P^0 pockets of the PSD-95 PDZ1-2 domain. The location of the fragments into P^0 was confirmed for **5**, **8**, and **9** by ^{1}H−^{15}N HSQC NMR. Several derivatives of **8** were made, which gave insight into the structural requirements for affinity, confirmed the suggested docking pose, and provided equipotent analogues thereby guiding future optimizations.

This work is one of the rare examples of successful fragment screening studies related to a PDZ domain target[24] and to the best of our knowledge the only one related to PSD-95. We show that indeed it is possible to find ligand efficient fragments against PDZ1-2 of PSD-95 by screening a commercial fragment library using a well-optimized biochemical assay followed by thorough counter-tests and biophysical assessments. The nature of the target – especially the small size of the main hydrophobic pocket and the lack of closely related secondary pockets – makes optimization very challenging. However, combining peptidomimetic strategies with the insight and results obtained from this study could perhaps facilitate the development of more potent PSD-95 inhibitors with useful drug-like properties.

Table 2. SPR activity of analogues of **8**[a]

F#	Structure	SPR (K_d/mM)	F#	Structure	SPR (K_d/mM)	F#	Structure	SPR (K_d/mM)
10		Very weak	17		Very weak	24		Very weak
11		12	18		No binding	25		7.0
12		No binding	19		No binding	26		9.6
13		Very weak	20		Very weak	27		8.4
14		Very weak	21		No binding	28		8.6
15		Very weak	22		No binding	29		6.1
16		Very weak	23		No binding			

[a] Compounds were tested by dose-response multi-cycle injections (MCI) in 2-fold serial dilutions (125 µM – 2 mM) (n=1). A confirmatory OneStep injection (1 mM) experiment was also conducted (n=1, not shown). K_d values are determined from steady-state affinity analysis by fitting to a 1:1 model and by fixing Rmax to the value of control peptide **3**. K_d values were determined for compounds showing dose-dependent responses across all tested concentrations. Compounds where only 1–2 of the highest concentrations led to responses >2 RU are designated 'Very weak'. And those only showing responses <2 RU are termed 'No binding'.

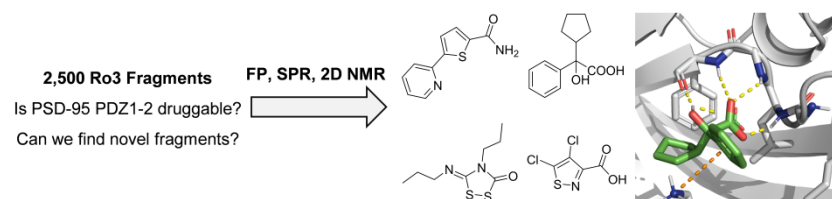[1] R. Sattler, Z. Xiong, W. Y. Lu, M. Hafner, J. F. MacDonald, M. Tymianski, *Science* **1999**, *284*, 1845-1848.

[2] M. Aarts, Y. Liu, L. Liu, S. Besshoh, M. Arundine, J. W. Gurd, Y. T. Wang, M. W. Salter, M. Tymianski, *Science* **2002**, *298*, 846-850.

[3] a) D. J. Cook, L. Teves, M. Tymianski, *Nature* **2012**, *483*, 213-217; b) M. D. Hill, R. H. Martin, D. Mikulis, J. H. Wong, F. L. Silver, K. G. Terbrugge, G. Milot, W. M. Clark, R. L. Macdonald, M. E. Kelly, M. Boulton, I. Fleetwood, C. McDougall, T. Gunnarsson, M. Chow, C. Lum, R. Dodd, J. Poublanc, T. Krings, A. M. Demchuk, M. Goyal, R. Anderson, J. Bishop, D. Garman, M. Tymianski, E. t. investigators, *Lancet Neurol.* **2012**, *11*, 942-950; c) M. D. Hill, M. Goyal, B. K. Menon, R. G. Nogueira, R. A. McTaggart, A. M. Demchuk, A. Y. Poppe, B. H. Buck, T. S. Field, D. Dowlatshahi, B. A. van Adel, R. H. Swartz, R. A. Shah, E. Sauvageau, C. Zerna, J. M. Ospel, M. Joshi, M. A. Almekhlafi, K. J. Ryckborst, M. W. Lowerison, K. Heard, D. Garman, D. Haussen, S. M. Cutting, S. B. Coutts, D. Roy, J. L. Rempel, A. C. Rohr, D. Iancu, D. J. Sahlas, A. Y. X. Yu, T. G. Devlin, R. A. Hanel, V. Puetz, F. L. Silver, B. C. V. Campbell, R. Chapot, J. Teitelbaum, J. L. Mandzia, T. J. Kleinig, D. Turkel-Parrella, D. Heck, M. E. Kelly, A. Bharatha, O. Y. Bang, A. Jadhav, R. Gupta, D. F. Frei, J. W. Tarpley, C. G. McDougall,

COMMUNICATION

WILEY-VCH

S. Holmin, J. H. Rha, A. S. Puri, M. C. Camden, G. Thomalla, H. Choe, S. J. Phillips, J. L. Schindler, J. Thornton, S. Nagel, J. H. Heo, S. I. Sohn, M. N. Psychogios, R. F. Budzik, S. Starkman, C. O. Martin, P. A. Burns, S. Murphy, G. A. Lopez, J. English, M. Tymianski, ESCAPE-NA1 Investigators, *Lancet* **2020**, *395*, 878-887.

[4] a) A. Bach, B. H. Clausen, M. Møller, B. Vestergaard, C. N. Chi, A. Round, P. L. Sørensen, K. B. Nissen, J. S. Kastrup, M. Gajhede, P. Jemth, A. S. Kristensen, P. Lundström, K. L. Lambertsen, K. Strømgaard, *Proc. Natl. Acad. Sci. U. S. A.* **2012**, *109*, 3317-3322; b) A. Bach, B. H. Clausen, L. K. Kristensen, M. G. Andersen, D. G. Ellman, P. B. L. Hansen, H. Hasseldam, M. Heitz, D. Ozcelik, E. J. Tuck, M. V. Kopanitsa, S. G. N. Grant, K. Lykke-Hartmann, F. F. Johansen, K. L. Lambertsen, K. Strømgaard, *Neuropharmacology* **2019**, *150*, 100-111.

[5] a) F. Tao, Q. Su, R. A. Johns, *Mol Ther* **2008**, *16*, 1776-1782; b) B. W. LeBlanc, M. Iwata, A. P. Mallon, C. N. Rupasinghe, D. J. Goebel, J. Marshall, M. R. Spaller, C. Y. Saab, *Neuroscience* **2010**, *167*, 490-500; c) R. D'Mello, F. Marchand, S. Pezet, S. B. McMahon, A. H. Dickenson, *Mol. Ther.* **2011**, *19*, 1780-1792.

[6] L. M. Ittner, Y. D. Ke, F. Delerue, M. Bi, A. Gladbach, J. van Eersel, H. Wolfing, B. C. Chieng, M. J. Christie, I. A. Napier, A. Eckert, M. Staufenbiel, E. Hardeman, J. Gotz, *Cell* **2010**, *142*, 387-397.

[7] F. X. Soriano, M. A. Martel, S. Papadia, A. Vaslin, P. Baxter, C. Rickman, J. Forder, M. Tymianski, R. Duncan, M. Aarts, P. Clarke, D. J. Wyllie, G. E. Hardingham, *J. Neurosci.* **2008**, *28*, 10696-10710.

[8] a) C. N. Chi, A. Bach, K. Strømgaard, S. Gianni, P. Jemth, *BioFactors* **2012**, *38*, 338-348; b) N. R. Christensen, J. Calyseva, E. F. A. Fernandes, S. Luchow, L. S. Clemmensen, L. M. Haugaard-Kedström, K. Strømgaard, *Adv. Ther.* **2019**, *2*, 1800143.

[9] a) E. Y. S. Lin, L. F. Silvian, D. J. Marcotte, C. C. Banos, F. Jow, T. R. Chan, R. M. Arduini, F. Qian, D. P. Baker, C. Bergeron, C. A. Hession, R. L. Huganir, C. F. Borenstein, I. Enyedy, J. Zou, E. Rohde, M. Wittmann, G. Kumaravel, K. J. Rhodes, R. H. Scannevin, A. Dunah, K. M. Guckian, *Sci. Rep.* **2018**, *8*; b) D. J. Marcotte, J. C. Hus, C. C. Banos, C. Wildes, R. Arduini, C. Bergeron, C. A. Hession, D. P. Baker, E. Lin, K. M. Guckian, A. W. Dunah, L. F. Silvian, *Protein Sci.* **2018**, *27*, 672-680.

[10] A. Bach, T. B. Pedersen, K. Strømgaard, *MedChemComm* **2016**, *7*, 531-536.

[11] a) D. C. Fry, L. T. Vassilev, *J. Mol. Med.* **2005**, *83*, 955-963; b) P. J. Hajduk, J. R. Huth, S. W. Fesik, *J. Med. Chem.* **2005**, *48*, 2518-2525.

[12] M. A. Stiffler, J. R. Chen, V. P. Grantcharova, Y. Lei, D. Fuchs, J. E. Allen, L. A. Zaslavskaia, G. MacBeath, *Science* **2007**, *317*, 364-369.

[13] a) D. Kozakov, D. R. Hall, R. L. Napoleon, C. Yueh, A. Whitty, S. Vajda, *J. Med. Chem.* **2015**, *58*, 9063-9088; b) D. Kozakov, L. E. Grove, D. R. Hall, T. Bohnuud, S. E. Mottarella, L. Luo, B. Xia, D. Beglov, S. Vajda, *Nat. Protoc.* **2015**, *10*, 733-755.

[14] A. Bach, C. N. Chi, T. B. Olsen, S. W. Pedersen, M. U. Røder, G. F. Pang, R. P. Clausen, P. Jemth, K. Strømgaard, *J. Med. Chem.* **2008**, *51*, 6450-6459.

[15] M. Congreve, R. Carr, C. Murray, H. Jhoti, *Drug Discov. Today* **2003**, *8*, 876-877.

[16] K. B. Nissen, L. M. Haugaard-Kedstrom, T. S. Wilbek, L. S. Nielsen, E. Aberg, A. S. Kristensen, A. Bach, P. Jemth, K. Strømgaard, *PloS One* **2015**, *10*, e0117668.

[17] K. T. Tran, J. S. Pallesen, S. M. Ø. Solbak, D. Narayanan, A. Baig, J. Zang, A. Aguayo-Orozco, R. M. C. Carmona, A. D. Garcia, A. Bach, *J. Med. Chem.* **2019**, *62*, 8028-8052.

[18] S. L. McGovern, E. Caselli, N. Grigorieff, B. K. Shoichet, *J. Med. Chem.* **2002**, *45*, 1712-1722.

[19] S. M. Ø. Solbak, J. Zang, D. Narayanan, L. J. Høj, S. Bucciarelli, C. Softley, S. Meier, A. E. Langkilde, C. H. Gotfredsen, M. Sattler, A. Bach, *J. Med. Chem.* **2020**, *63*, 1156-1177.

[20] A. Bach, C. N. Chi, G. F. Pang, L. Olsen, A. S. Kristensen, P. Jemth, K. Strømgaard, *Angew. Chem. Int. Ed.* **2009**, *48*, 9685-9689.

[21] A. M. Giannetti, H. N. Gilbert, D. P. Huddler, M. Reiter, C. Strande, K. E. Pitts, B. J. Bravo in *Fragment-Based Drug Discovery* (Royal Society of Chemistry), **2015**, pp. 19-48.

[22] S. W. Pedersen, S. B. Pedersen, L. Anker, G. Hultqvist, A. S. Kristensen, P. Jemth, K. Strømgaard, *Nat. Commun.* **2014**, *5*, 3215.

[23] A. L. Hopkins, C. R. Groom, A. Alex, *Drug Discov. Today* **2004**, *9*, 430-431.

[24] a) T. P. Kegelman, B. Wu, S. K. Das, S. Talukdar, J. M. Beckta, B. Hu, L. Emdad, K. Valerie, D. Sarkar, F. B. Furnari, W. K. Cavenee, J. Wei, A. Purves, S. K. De, M. Pellecchia, P. B. Fisher, *Proc. Natl. Acad. Sci. U. S. A.* **2017**, *114*, 370-375; b) M. Joshi, C. Vargas, P. Boisguerin, A. Diehl, G. Krause, P. Schmieder, K. Moelling, V. Hagen, M. Schade, H. Oschkinat, *Angew. Chem. Int. Ed.* **2006**, *45*, 3790-3795.

6

COMMUNICATION   **WILEY**-VCH

Entry for the Table of Contents

PDZ domains are intriguing but challenging drug targets. Here, we investigate the druggability of PDZ1-2 of PSD-95 by a computational method and fragment-based screening using biochemical and biophysical assays. This results in new well validated fragments shown to bind the PDZ domains of PSD-95.

Institute and/or researcher Twitter usernames: @group_bach; @UCPH_health